Variability Impact of Many Design Parameters: The Case of a Realistic Electronic Link

Variability Impact of Many Design Parameters: the Case of a Realistic Electronic Link

Mourad Larbi, Igor S. Stievano, *Senior Member, IEEE,* Flavio G. Canavero, *Fellow, IEEE,* and Philippe Besnier, *Senior Member, IEEE*

***Abstract*— In this paper, we adopt the so-called sparse polynomial chaos metamodel for the uncertainty quantification in the framework of high-dimensional problems. This metamodel is used to model a realistic electronic bus structure with a large number of uncertain input parameters such as those related to microstrip line geometries. It aims at estimating quantities of interest, such as statistical moments, probability density functions and provides sensitivity analysis of a response. It drastically reduces the model computational cost with regard to brute force Monte Carlo (MC) simulation. The method presents a good performance and is validated in comparison with MC simulation.**

***Index Terms*— Circuit design, crosstalk, discontinuities, high dimensional problems, risk analysis, sparse polynomial chaos, uncertainty quantification.**

I. Introduction

Various electronic systems are encountered in everyday life, at all size, complexity and throughput levels. They consist of collections of electronic and electrical parts interconnected to perform specific tasks. A good example is the automobile electrical system, that has gradually evolved over the years from a simple power distribution network to currently assimilate automatic computer control of the automotive mechanics. A key characteristic of electronic systems is, that the individual components are interconnected with wires or printed circuit boards. Signals flowing inside the system travel across transmission lines sections of different types and shapes, encounter connectors, sockets, vias, and transitions that act as discontinuities with complex electromagnetic behavior and are influenced by many different parameters. Most of them may be considered as uncertain parameters due to the fabrication process, the materials used, the dependence on temperature, etc. The analysis of signal links is therefore a challenging task, and the design must be optimized toward the reduction of the impact of the numerous geometric and material uncertainties on the system signal integrity (SI) and electromagnetic compatibility (EMC).

In the past decade, some research activities have been dedicated to the estimation of statistical quantities in the framework of high-speed interconnects [1]–[3] or wiring applications [4]–[6]. Among them, the so-called polynomial chaos (PC) has been successfully introduced to substitute a costly model by an analytic approximation called metamodel (or surrogate model). This metamodel is built up from a reduced number of calls to the initial model. The advantage of using the metamodel stems from the reduced computational effort needed for the statistical assessment of output quantities, like the estimation of statistical moments or probability density functions (PDF). Nonetheless, as the number of uncertain parameters increases, the number of required polynomials blows up as well as the number of calls to the numerical model. This problem, referred to as the *curse of dimensionality*, requires the adoption of an alternative technique based on a *sparse* PC approximation [7], devised to select the polynomials contributing the most to the model. We highlight that the sparse PC approximation makes possible the analysis of complex electric interconnections with impedance discontinuities introduced by vias or sockets on printed circuit boards (PCBs). The paper is then organized as follows. Section II presents the method, while Section III describes the case study used, which is a realistic node-to-node bus with a high number of uncertain parameters, and provides and discusses the results obtained by the sparse PC metamodel.

M. Larbi, I.S. Stievano and F. G. Canavero are with the Dipartimento di Elettronica e Telecomunicazioni, EMC Group, Politecnico di Torino, Torino 10129, Italy (e-mail: mourad.larbi@polito.it; igor.stievano@polito.it; flavio.canavero@polito.it).

P. Besnier is with the Institut d'Électronique et de Télécommunications de Rennes (IETR), UMR CNRS 6164, INSA de Rennes, Rennes 35043, France (e-mail: philippe.besnier@insa-rennes.fr).

II. Polynomial Chaos Expansion

A. Introduction

Let us consider a random vector $\boldsymbol{X}$ of M independent random variables $(X_1, \ldots, X_M)$ with a joint PDF $f_{\boldsymbol{X}}(\boldsymbol{x})$ characterizing the input uncertainties of the physical system. The random response of the system, assumed to be scalar with a finite variance, is defined by $Y = \mathcal{M}(\boldsymbol{X})$, where $\mathcal{M}$ is a numerical model representing the observed phenomenon.

The PC expansion of the model response is then given by [8]:

$$Y = \sum_{\boldsymbol{\lambda} \in \mathbb{N}^M} a_{\boldsymbol{\lambda}} \Phi_{\boldsymbol{\lambda}}(\boldsymbol{X}), \tag{1}$$

where $a_{\boldsymbol{\lambda}}$ are unknown coefficients defining the coordinates of Y in the new basis $\Phi_{\boldsymbol{\lambda}}$ of multivariate polynomials, which are orthonormal with respect to the joint PDF $f_{\boldsymbol{X}}(\boldsymbol{x})$.

In order to compute the $a_{\boldsymbol{\lambda}}$ coefficients, various non-intrusive methods such as the approaches by projection

and regression may be used [9]. Since the convergence of the regression method is quicker in terms of calls to the numerical model $\mathcal{M}$, we present it in the next section.

B. Non-intrusive Estimation of the Coefficients by Regression

Let $\boldsymbol{\mathcal{X}} = \{\boldsymbol{x}^{(1)}, \ldots, \boldsymbol{x}^{(n)}\}$ and $\mathcal{Y} = \{\mathcal{M}(\boldsymbol{x}^{(1)}), \ldots, \mathcal{M}(\boldsymbol{x}^{(n)})\}$ be an *experimental design* (ED) of $\boldsymbol{X}$ and the associated model responses, respectively. From the set of model evaluations $\mathcal{Y}$, the PC coefficients can be estimated by the ordinary least square regression [10]. For this, the infinite series in (1) has to be truncated. Choosing a maximum polynomial degree l, the usual truncation scheme preserves all polynomials associated to the set $\mathcal{A}^{M,l} = \{\boldsymbol{\lambda} \in \mathbb{N}^M : \|\boldsymbol{\lambda}\|_1 = \sum_{i=1}^{M} \lambda_i \leq l\}$. Thus, the cardinal of the set $\mathcal{A}^{M,l}$ denoted $L = \dfrac{(M+l)!}{M!l!}$ increases quickly with the number of input random variables M and the degree l of the polynomials.

C. Sparse Polynomial Chaos Expansion

1) Hyperbolic Truncation Strategy: As mentioned above, the standard truncation scheme of the PC expansion preserves L elements included in the set $\mathcal{A}^{M,l}$. Another technique called as the *hyperbolic truncation scheme* has been introduced in [7] to significantly reduce the number of unknown terms when the dimensionality of the input space M is large. Let us introduce for any multi-index $\boldsymbol{\lambda}$, the k-norm $(0 < k \leq 1)$ defined as $\|\boldsymbol{\lambda}\|_k = \left(\sum_{i=1}^{M} \lambda_i^k\right)^{1/k}$.

The hyperbolic truncation strategy consists in retaining all multi-indices of k-norm less than or equal to the degree l as:

$$\mathcal{A}^{M,l,k} = \{\boldsymbol{\lambda} \in \mathbb{N}^M : \|\boldsymbol{\lambda}\|_k \leq l\}. \tag{2}$$

This hyperbolic truncation scheme favors the main effects and low-interactions polynomials, known to be the most influential on the variability of the model response due to the *sparsity-of-effect principle* [11]. An illustration of this hyperbolic truncation scheme for two input random variables ($M = 2$) is given in Fig. 1. The blue and pink points represent all terms of the polynomial basis of degree less than or equal to l, contained in the set (2). When $k = 1$, this corresponds to the standard truncation set $\mathcal{A}^{M,l}$, *i.e.* the blue points. When $k < 1$, the number of retained polynomials, *i.e.* the pink points, is smaller than in the standard truncation set $\mathcal{A}^{M,l}$. Indeed, the benefit is more and more significant in terms of reduction of the basis size when k decreases and M increases, as shown *e.g.* with $k = 0.5$ in Fig. 1. With this strategy, the size of the polynomial basis may be smaller by several orders of magnitude than that of the standard truncation scheme [7].

2) Adaptive Least Angle Regression Algorithm: The hyperbolic truncation strategy $\mathcal{A}^{M,l,k}$ enables to decrease the number of coefficients to be estimated in the PC expansion. However, this is still too expensive in terms of model evaluations when dealing with high dimensional problems. Thereby, a further reduction of the basis size can be carried out by using an adaptive technique such as the so-called Least Angle Regression (LARS) algorithm. LARS is only briefly described in the following paragraph. For more details readers may refer to [7], [12]. This method allows to select in the truncation set $\mathcal{A}^{M,l,k}$, say of cardinal K, the polynomial bases having the most effect on the response.

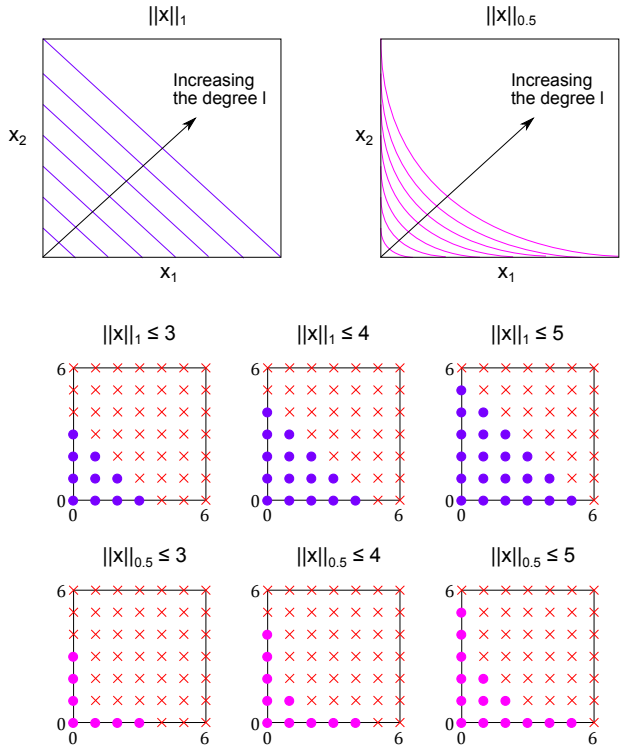

Fig. 1. Illustration of the hyperbolic truncation strategy for $k = 1$ and $k = 0.5$ in blue and pink points, respectively [7].

Among the K polynomial bases (associated to a given degree l), LARS builds up in an iterative manner a sparse representation containing from 1 to K polynomial bases according to their decreasing impact. The algorithm begins by researching the most correlated basis $\Phi_{\boldsymbol{\lambda}_1}$ with the response Y. In practice, the correlation is computed from a set of realizations of the bases $\Phi_{\boldsymbol{\lambda}}$'s and of the response $\mathcal{Y}$. Once the first polynomial basis $\Phi_{\boldsymbol{\lambda}_1}$ is obtained, the corresponding coefficient is estimated so way that the residual $Y - a_{\boldsymbol{\lambda}_1^{(1)}} \Phi_{\boldsymbol{\lambda}_1}(\boldsymbol{X})$ becomes equi-correlated with the polynomial basis $(\Phi_{\boldsymbol{\lambda}_1}, \Phi_{\boldsymbol{\lambda}_2})$. This first step will select the best first element of the basis. Then the improving of the basis is carried out by moving along the direction $(\Phi_{\boldsymbol{\lambda}_1} + \Phi_{\boldsymbol{\lambda}_2})$ until the current residual becomes equi-correlated with a third polynomial basis $\Phi_{\boldsymbol{\lambda}_3}$, and so on.

Finally, the LARS algorithm provides a set of sparse approximations containing more and more polynomial terms. The leave-one-out cross validation error ϵ_{LOO} of

each approximation is computed by:

$$\epsilon_{LOO} = \frac{\sum_{i=1}^{N} \left(\mathcal{M}(\boldsymbol{x}^{(i)}) - \mathcal{M}_{-i}^{PC}(\boldsymbol{x}^{(i)})\right)^2}{\sum_{i=1}^{N} \left(\mathcal{M}(\boldsymbol{x}^{(i)}) - \frac{1}{N}\sum_{i=1}^{N} \mathcal{M}(\boldsymbol{x}^{(i)})\right)^2} \quad (3)$$

with $\mathcal{M}_{-i}^{PC}(\boldsymbol{x}^{(i)})$ representing N sparse approximations built up on the ED $\boldsymbol{\mathcal{X}} \backslash \boldsymbol{x}^{(i)} = \{\boldsymbol{x}^{(j)}, j = 1, \ldots, N,\ j \neq i\}$. The sparse representation that provides the smallest error is selected. This procedure is repeated for each degree $l = 1, \ldots, l_{max}$, and the optimal sparse PC metamodel is retained from a leave-one-out cross validation error [7]. The main advantage of LARS is, that it enables to deal with problems whose number of candidate polynomial terms is larger than the size of the ED $\boldsymbol{\mathcal{X}}$. In general, the number of polynomial terms identified is less than the size of the ED $\boldsymbol{\mathcal{X}}$, which allows to estimate the coefficients of the sparse approximation by least-square minimization for improving the accuracy. In the rest of this article, the quality of the sparse PC approximation will be evaluated by means of the Q^2 coefficient defined by $Q^2 = 1 - \epsilon_{LOO}$, with $0 \leq Q^2 \leq 1$. Thus, the closer is Q^2 to 1, the higher is the quality of the sparse PC approximation.

D. Post-processing

One of the main advantages of the (sparse) PC representation is that it allows, after the computation of the PC coefficients, to derive a post-processing of the model response at a negligible computational cost. In particular, the orthonormal property of the polynomial basis enables to obtain the first two statistical moments of the output Y as:

$$\mathbb{E}[Y] = a_{\mathbf{0}} \quad (4)$$

$$\mathbb{V}[Y] = \sum_{\boldsymbol{\lambda} \in \mathcal{A} \backslash \{\mathbf{0}\}} a_{\boldsymbol{\lambda}}^2 \quad (5)$$

Further, [13] showed that the *first order PC-based Sobol indices* S_i of the model response Y with respect to the input random variable X_i can be estimated as:

$$S_i = \frac{\sum_{\boldsymbol{\lambda} \in \mathcal{A}_i} a_{\boldsymbol{\lambda}}^2}{\mathbb{V}[Y]} \quad (6)$$

with $\mathcal{A}_i = \{\boldsymbol{\lambda} \in \mathcal{A} : \lambda_i > 0, \lambda_j = 0 \quad \forall j \neq i\}$. The *total PC-based Sobol indices* $S_{T,i}$ can be also formulated as:

$$S_{T,i} = \frac{\sum_{\boldsymbol{\lambda} \in \mathcal{A}_{T,i}} a_{\boldsymbol{\lambda}}^2}{\mathbb{V}[Y]} \quad (7)$$

where $\mathcal{A}_{T,i} = \{\boldsymbol{\lambda} \in \mathcal{A} : \lambda_i \neq 0\}$.

III. Impact of Uncertainties in a Transmission Line Network

A. Description of the Bus Structure and the Circuit

In order to evaluate the impact of input uncertainties on signal propagation, in this section we consider the realistic bus structure described in Fig. 2. It involves the point-to-point communication between a driver and a receiver represented by the gray boxes in the bottom part of the schematic through a number of discontinuities.

The details of the equivalent electrical network, including various types of lines, vias, sockets and a strait, are illustrated in Fig. 3. The above example is inspired by the validation test case of [14], where the single PCB traces are replaced by the coupling blocks PCB_1 and PCB_2 in Fig. 3. These blocks consist of the combination of single (S_i) and coupled microstrip (C_j) transmission lines, the latter ones accounting for the interaction with other traces located on the PCB. The aim of this modification is twofold: on the one hand, the structure of Fig. 2 provides a more complex test case with an increased size and a larger number of uncertain parameters; on the other hand, it represents a possible realistic situation in which the main communication bus is close to neighboring lines, leading to mutual interference.

The MCM-C (multi-chip module with ceramic substrate) single lines of the network, denoted by M_1 and M_2 in the scheme, are modeled as identical 4 cm single microstrip lines, the socket is modeled by lumped elements, and the strait is modeled by a 8 cm single microstrip line (denoted as S_5) with two capacitors (C_4 and C_{10}) representing the end discontinuities. Besides, the receiver side of the main bus involves the same transitions already observed in the left-hand (i.e. driver) side, defined by the cascade connection of the top via TV_2, of the MCM-C single line M_2 and of the block labeled as BLL_{31} in the scheme. Moreover, the structure used for BLL_{31} is also used for the other terminations of the PCB coupled lines. This assumption of symmetry is done for the sake of simplicity in order to define a single modular receiving block in our simulating test bench (see BLL_{pq} in Fig. 3). The driver is modeled by means of a simplified Thevenin equivalent defined by the connection of the ideal voltage source V_1 and its series impedance (i.e., the resistor $R_1 = 30\,\Omega$). A frequency-domain analysis is carried out over the band [1 MHz - 1 GHz].

It is important to remark that the above described test structure involves vias of short length, thus justifying their modeling as lumped elements. Specifically, this holds for both the top and the bottom vias which are described as lumped LC elements, with $L = 4.457$ nH/cm, $C = 1.273$ pF/cm, and $L = 5.51$ nH/cm, $C = 1.03$ pF/cm, respectively. The values of the cross section parameters of the PCB and MCM-C traces, which are modeled as ideal lossless transmission lines, are shown in Fig. 4 instead.

The variability of the structure is introduced through all cross section parameters of the different lines (MCM-C, single and coupled microstrip lines) and all lumped elements of the network, which are considered as uniform random variables with uncertainty of 20 % around their nominal values given in Fig. 4 and Fig. 3, respectively. The total number of uncertain parameters turns out to be 119. The impact of these uncertain input parameters will be evaluated on the frequency-domain crosstalk transfer function magnitude $H_{11} = 20 \times \log \left| \frac{V_{11}}{V_1} \right|$ dB, defined as the ratio between the far-end voltage of the block BLL_{11} and the voltage excitation. The crosstalk transfer function

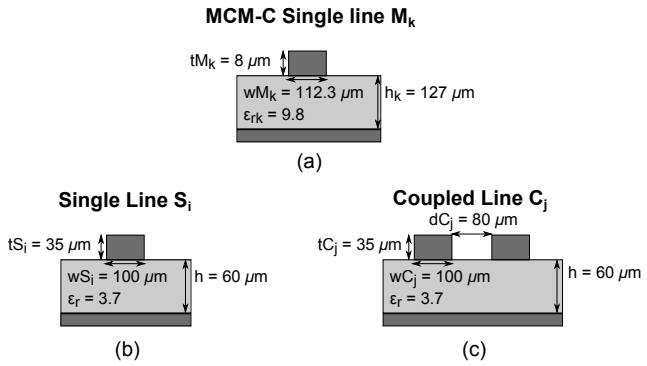

Fig. 4. Cross section of the (a) ceramic multi-chip module (MCM-C); (b) single and (c) coupled microstrip lines.

H_{11} is numerically computed for the circuit model of Fig. 3 which we denote by $\mathcal{M}$ in the following. For convenience, MATLAB is used for the frequency evaluation of $\mathcal{M}$, but a SPICE solution of the circuit could have been used, instead, with equivalent results.

The purpose of the study is to build up a sparse PC metamodel of the crosstalk transfer function H_{11} in order to reduce the computational cost of the numerical model. Furthermore, we are particularly interested in assessing the rank of the uncertain parameters according to their influence on the variability of the crosstalk transfer function.

B. Numerical Analysis and Discussion

The results given in this section were obtained by means of the UQLAB toolbox (Uncertainty Quantification toolbox in MATLAB) [15].

1) Sparse Polynomial Chaos Representation of the Model Response: This section examines the effect of input uncertainties on the crosstalk transfer function H_{11} over the frequency band [1 MHz - 1 GHz]. Thereby, we approximate the model response by building up a sparse PC expansion with 200 realizations from Latin Hypercube Sampling (LHS) [16] and an adaptive degree l varying from 1 to 10. The degree span selected is quite large since the crosstalk transfer function H_{11} can be very irregular in the frequency domain where the resonance effects occur. Given the high number of input random variables, the k parameter defined in (2) is set to 0.4 in order to considerably reduce the size of the polynomial basis.

In order to observe the quality of the sparse PC metamodel built up, we represent in Fig. 5 the Q^2 coefficient over the frequency band [1 MHz - 1 GHz]. A sparse PC metamodel is determined for 301 logarithmically spaced frequencies. We see that the sparse PC metamodel has a high quality in the frequency band [1 MHz - 400 MHz], and then it fluctuates in the frequency band [400 MHz - 1 GHz], from 0.3 (low quality) to around 0.95 (good quality). This latter behavior of the Q^2 coefficient is likely due to important variations of the crosstalk transfer function H_{11} in the resonance regime. To confirm this, we represent in Fig. 6, three Monte Carlo (MC) realizations of the crosstalk transfer function H_{11} computed by the sparse PC metamodel $\mathcal{M}^{PC}(\boldsymbol{x}^{(i)})$ (circles) and by the numerical model $\mathcal{M}(\boldsymbol{x}^{(i)})$ (solid line). We observe that the two models are in agreement in the low frequency domain [1 MHz - 400 MHz]; some discrepancies appear between 400 MHz and 1 GHz, in the region where the resonances influence the response H_{11}. This is related to the smooth evolution as well as the strong variations of the crosstalk transfer function H_{11} in low and high frequency domain, respectively.

We are now interested in evaluating the accuracy of this sparse PC metamodel in low and in high frequency, *e.g.* at the frequencies of 10 MHz and 912 MHz, where $Q^2_{10\text{ MHz}} = 99.80\%$ and $Q^2_{912\text{ MHz}} = 89.42\%$. To do so, we represent, from 10000 MC realizations, the PDF of the crosstalk transfer function H_{11} given by sparse PC metamodel (red dashed-line) and by MC simulation (blue solid line) at the frequencies of 10 MHz and of 912 MHz in Fig. 7(a) and in Fig. 7(b), respectively. In Fig. 7(a), we observe a quasi-perfect agreement of the two curves, highlighting a very good accuracy of the sparse PC metamodel at 10 MHz. Concerning the mean and the standard deviation of H_{11}, they are quite close since the sparse PC and the MC simulation provide $\mu^{PC} = -52.43$ dB, $\sigma^{PC} = 1.86$ dB and $\mu^{MC} = -52.46$ dB, $\sigma^{MC} = 1.90$ dB, respectively. The sparse PC approximation needs a best degree of order 6, with only 44 polynomial elements among the 7736 elements of the full polynomial basis, leading to the sparsity index $SI = \frac{44}{7736} = 0.57\%$.

Regarding the frequency of 912 MHz, we observe in Fig. 7(b) that the PDF retrieved from the sparse PC does not fit so well with the PDF estimated from MC simulations. In fact, the main trend of the PDF is captured by the sparse PC metamodel, but significant disagreement occurs at the tail of the probability distribution. For this frequency, the estimation of the mean and of the standard deviation given by the sparse PC and the MC simulation, provides $\mu^{PC} = -28.08$ dB, $\sigma^{PC} = 4.15$ dB and $\mu^{MC} = -28.13$ dB, $\sigma^{MC} = 4.80$ dB, respectively. The optimal degree used by the sparse PC metamodel is 10, with a sparsity index $SI = \frac{16}{22254} = 0.07\%$.

The results obtained by the sparse PC metamodel at these two frequencies provide interesting information on the behavior of H_{11}. Indeed, at 912 MHz, the sparse PC approximation is less accurate, and uses a larger optimal degree. This is related to a more important variability of H_{11}, as shown by the standard deviation $\sigma^{MC} = 4.80$ dB. Nonetheless, the sparsity index is smaller, meaning that only a few terms of the polynomial basis are needed to approximate the variability of the model response H_{11}. Concerning the CPU time required for the computation of the crosstalk transfer function H_{11} in the frequency band [1 MHz - 1 GHz], the sparse PC metamodel took 3.05 s while 10000 MC realizations needed 6 h 11 min. The speed up gain of the metamodel is then about 7308× compared to the MC method.

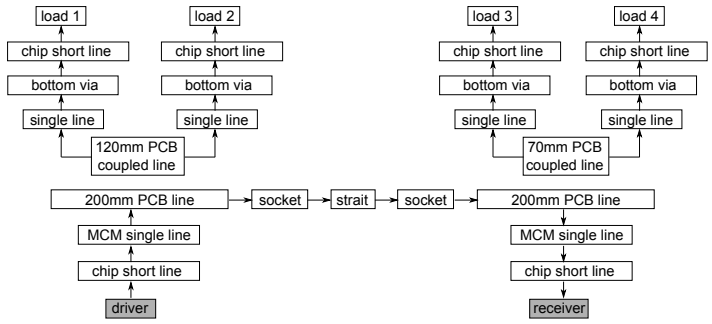

Fig. 2. High-level diagram of the node-to-node bus under study. The main electronic link goes from driver to receiver, while the loads 1-4 represent side circuits that may be affected by crosstalk.

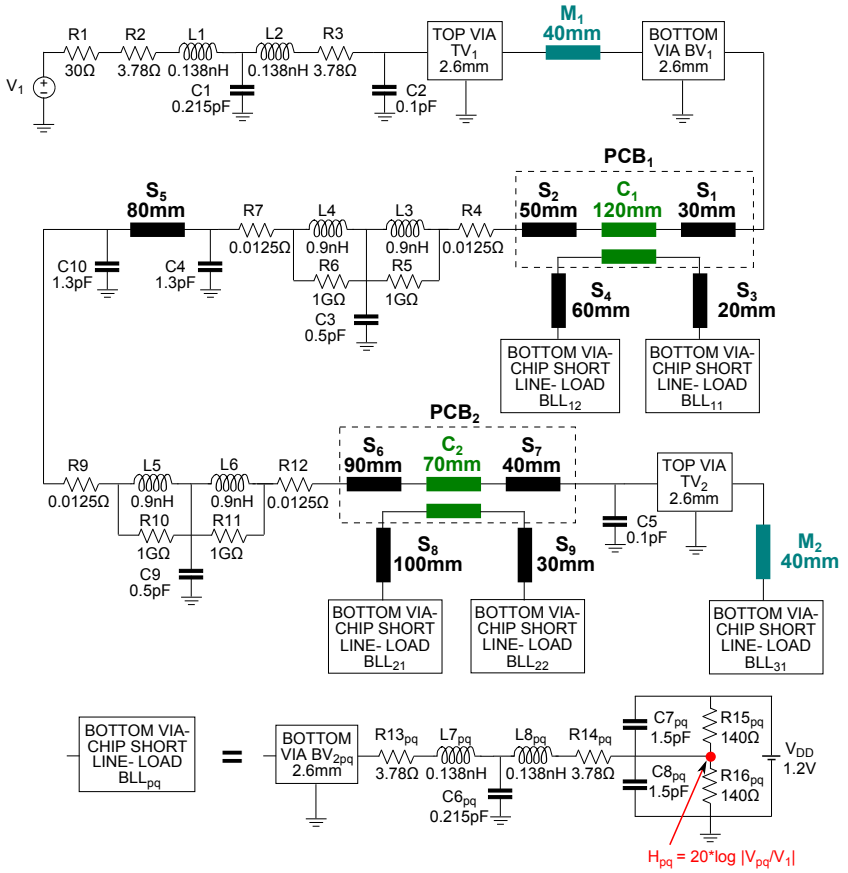

Fig. 3. Schematic of the node-to-node bus under study. Top and Bottom vias are represented as LC circuits with values specified in the text.

2) Sensitivity Analysis from Sobol Indices: Beyond the quantification of the variability of the crosstalk transfer function H_{11}, the sparse PC metamodel provides a sensitivity analysis of this latter at a low computational cost. In Fig. 8, we represent an histogram showing the maximum values of the total Sobol indices, calculated from (7), of the crosstalk transfer function H_{11} over the frequency band [1 MHz - 1 GHz]. Observing Fig. 8, we see that among the 119 input random variables, only 22 variables have a significant effect on the variability of H_{11} with maximum values of the total Sobol indices greater than 5% (red dashed-line). In particular, we notice that the variables having the greatest impact on the variations of H_{11} in the overall frequency band are the relative permittivity ϵ_r and the thickness h of the substrate, for all single and coupled microstrip lines of the network, and the trace-to-trace separation $dC1$ of the coupled line $C1$. Then, we observe that different cross section parameters, such as the trace widths $wC1$ and $wC2$, $wS2$, $wS4$ and $wS7$ of the coupled lines $C1$, $C2$ and single lines $S2$, $S4$, $S7$,

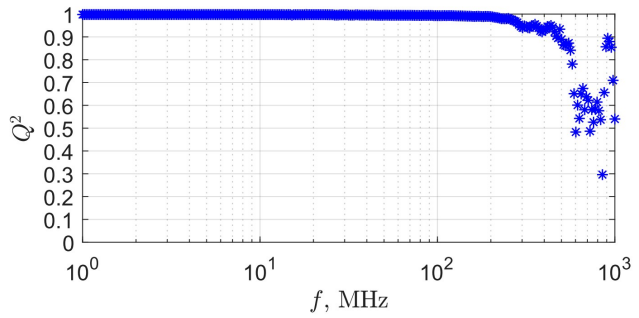

Fig. 5. Computation of the Q^2 coefficient of the sparse PC metamodel in the frequency band [1 MHz - 1 GHz].

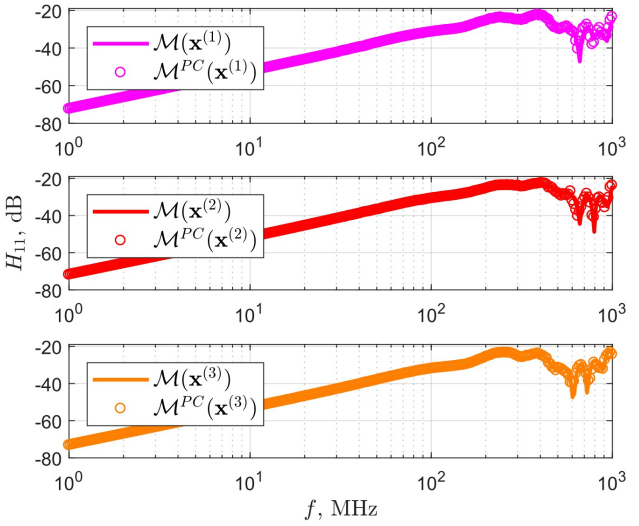

Fig. 6. Representation of the crosstalk transfer function H_{11} in the frequency band [1 MHz - 1 GHz] estimated by the sparse PC metamodel $\mathcal{M}^{PC}$ (circles) and the numerical model $\mathcal{M}$ (solid line) from three MC realizations.

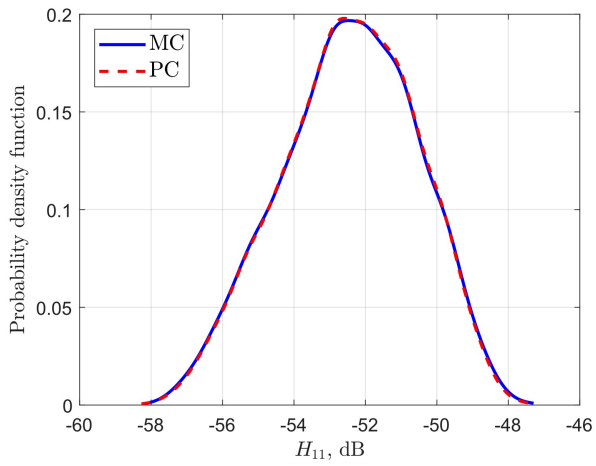

(a)

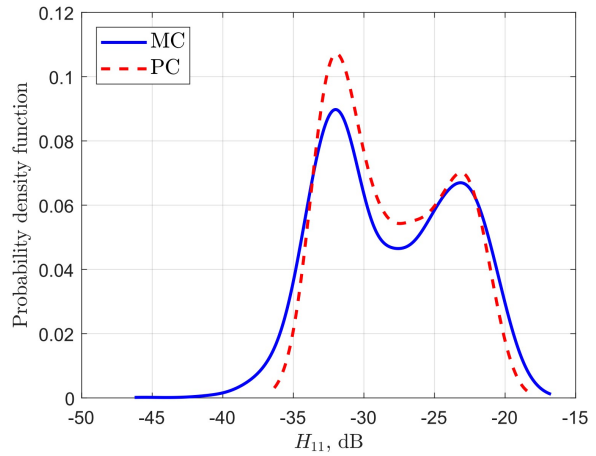

(b)

Fig. 7. PDF of the crosstalk transfer function H_{11} obtained by sparse PC (red dashed-line) and by MC simulation (blue solid line) at the frequencies of (a) 10 MHz and of (b) 912 MHz.

respectively, the trace thicknesses $tS3$, $tS6$, and $tS9$, and the substrate thickness $h2$ of the MCM-C single line $M2$, have less impact. Finally, we identify an effect with more or less the same order of magnitude as for the cross section parameters, due to several lumped elements of the network, *i.e.* $R1$, $L4$, $R7$, $C10$, $R10$, $R1522$, $C731$, and of top via lines, *i.e.* $CTV1$, $LTV2$, $CTV2$.

In order to illustrate the effect of all input random variables mentioned previously, we represent in Fig. 9 their total Sobol indices over the frequency band [1 MHz - 1 GHz]. From 1 MHz to 600 MHz, we see that the variations of the crosstalk transfer function H_{11} are mainly related to the substrate thickness h, the trace-to-trace separation $dC1$ and the trace width $wC1$ of the coupled line $C1$, the relative permittivity ϵ_r and the component $R1$. Moreover, we remark the occurrence of small impact of variables as the trace widths $wC2$, $wS4$, $wS7$, the substrate thickness $h2$ and the component $C10$. Then, from 600 MHz to 1 GHz, the relative permittivity ϵ_r is the predominant variable influencing the variability of H_{11}. Other variables, as for example $wC1$, $wC2$ $wS4$, $L4$, $R7$, $C10$, $CTV2$ and $LTV2$, have a small impact on the variations of H_{11}. It is also relevant to highlight the fact that a larger number of input variables is observed in this latter frequency band, likely because the resonance regime is more sensitive to numerous parameters constituting the transmission line network.

Otherwise, the sensitivity analysis shows that three uncertain parameters, *i.e.* the substrate thickness h, the trace-to-trace separation $dC1$ of the coupled line $C1$ and the substrate dielectric relative permittivity ϵ_r, have an important influence on the variations of the crosstalk transfer function H_{11} in the overall frequency band. It might be interesting to represent the effect of these uncertain parameters on the variability of H_{11}. Thus, by varying only the considered parameter between the minimum, mean and maximum value of their range, Fig. 10 illustrates the variation of H_{11}. In Fig. 10, we observe that the effect of a variation of the relative permittivity ϵ_r (top) has only an impact at high frequencies, with a variation of the magnitude levels and occurrence of the resonance

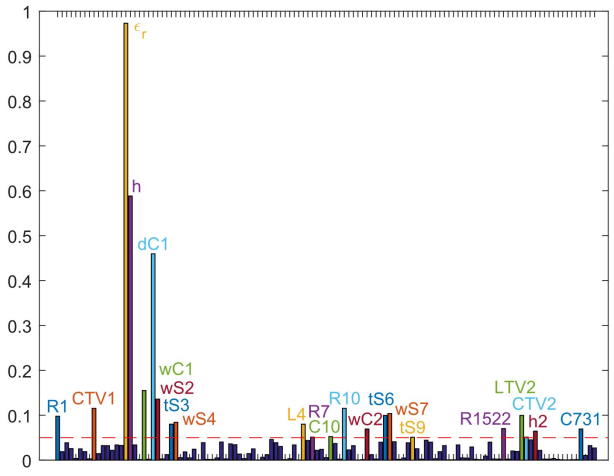

Fig. 8. Maximum values over the frequency band [1 MHz - 1 GHz] of total Sobol indices of the crosstalk transfer function H_{11}. The red dashed-line represents the selected 5% threshold for parameters impact.

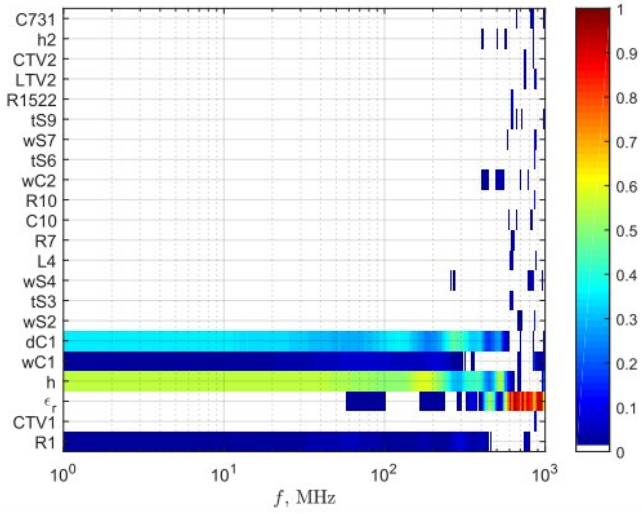

Fig. 9. Total Sobol indices of the crosstalk transfer function H_{11}, in the frequency band [1 MHz - 1 GHz].

peaks in [400 MHz - 1 GHz]. Concerning the substrate thickness h (middle) and the trace-to-trace separation $dC1$ of the coupled line $C1$ (bottom), the effect of their variations is much more important at low frequencies, *i.e.* [1 MHz - 400 MHz]. It is worth noting that the effect of the variations of these uncertain parameters is in total agreement with the sensitivity analysis given in Fig. 9.

IV. Conclusion

This paper presents a sparse PC metamodel, with a very low computational cost compared to MC simulation, for the analysis of signal propagation on realistic electronic buses with a large number of uncertain parameters. This sparse PC metamodel allowed to efficiently estimate the model output in a large part of the frequency band considered, where the response is rather smooth. When the

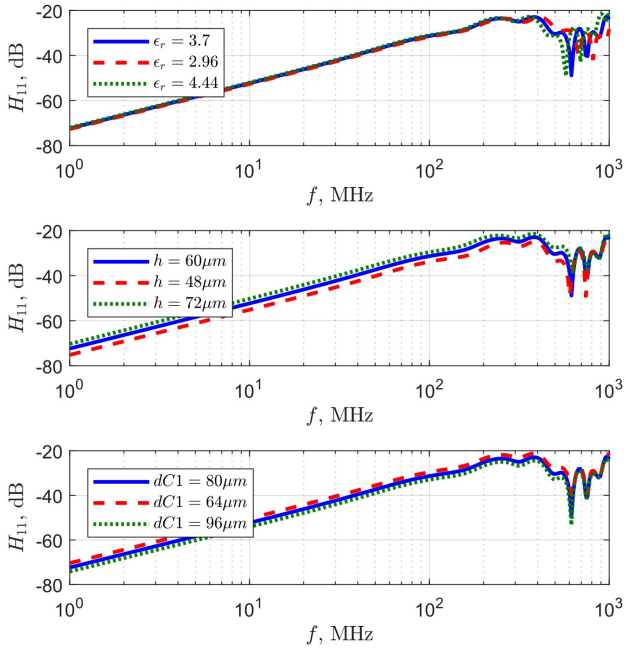

Fig. 10. Impact of a variation of the dielectric relative permittivity ϵ_r (top), the substrate thickness h (middle), and the trace-to-trace separation $dC1$ of the coupled line $C1$ (bottom) on the crosstalk transfer function H_{11}.

variations of the output become very important, as in the resonance regime, the predictions of the metamodel may be less accurate.

In addition to a good estimation of the first two statistical moments, the sparse PC metamodel provides also a sensitivity analysis of the model response at a low computational cost. From this sensitivity analysis, the designer of the circuit may identify the input uncertain variables having the largest influence on the variability of the output. This may lead to adapt more restrictive constraints on the predominant uncertain variables during the design stage, in order to improve the robustness of the design itself. Our case study with 119 uncertain input variables illustrates that the variability of the model response is often explained by a small group of uncertain input variables.

As mentioned previously, the estimations of the sparse PC metamodel may be inaccurate and sometimes insufficient at high frequencies, especially in the resonance region. This is often due to one uncertain input variable (such as the substrate relative permittivity) that generates strong variations of the model output. Thus, the metamodel user can sweep the uncertain parameter and gain a clear insight in the device behavior and properly tune the design to achieve higher performances.

References

[1] I. S. Stievano, P. Manfredi, and F. G. Canavero, "Parameters variability effects on multiconductor interconnects via hermite polynomial chaos," *IEEE Transactions on Components, Packaging and Manufacturing Technology*, vol. 1, no. 8, pp. 1234–1239, Aug. 2011.

[2] P. Manfredi and F. Canavero, "Numerical calculation of polynomial chaos coefficients for stochastic per-unit-length parameters of circular conductors," *Magnetics, IEEE Transactions on*, vol. 50, no. 3, pp. 74–82, Mar. 2014.

[3] Y. Tao, B. Nouri, M. Nakhla, and R. Achar, "Efficient time-domain variability analysis using parameterized model-order reduction," in *2016 IEEE 20th Workshop on Signal and Power Integrity (SPI)*, May 2016, pp. 1–4.

[4] M. Larbi, P. Besnier, and B. Pecqueux, "The adaptive controlled stratification method applied to the determination of extreme interference levels in emc modeling with uncertain input variables," *IEEE Transactions on Electromagnetic Compatibility*, vol. 58, no. 2, pp. 543–552, Apr. 2016.

[5] ——, "Probability of emc failure and sensitivity analysis with regard to uncertain variables by reliability methods," *Electromagnetic Compatibility, IEEE Transactions on*, vol. 57, no. 2, pp. 274–282, Apr. 2015.

[6] T. Bdour, C. Guiffaut, and A. Reineix, "Use of adaptive kriging metamodeling in reliability analysis of radiated susceptibility in coaxial shielded cables," *IEEE Transactions on Electromagnetic Compatibility*, vol. 58, no. 1, pp. 95–102, Feb. 2016.

[7] G. Blatman and B. Sudret, "Adaptive sparse polynomial chaos expansion based on least angle regression," *Journal of Computational Physics*, vol. 230, no. 6, pp. 2345–2367, 2011.

[8] C. Soize and R. Ghanem, "Physical systems with random uncertainties: chaos representations with arbitrary probability measure," *SIAM Journal on Scientific Computing*, vol. 26, no. 2, pp. 395–410, 2004.

[9] B. Sudret, "Uncertainty propagation and sensitivity analysis in mechanical models–contributions to structural reliability and stochastic spectral methods," Habilitation à diriger des recherches, Université Blaise Pascal, Clermont-Ferrand, France, Oct. 2007.

[10] M. Berveiller, B. Sudret, and M. Lemaire, "Stochastic finite element: a non intrusive approach by regression," *European Journal of Computational Mechanics*, vol. 15, no. 1-3, pp. 81–92, 2006.

[11] D. C. Montgomery, *Design and analysis of experiments*. John Wiley & Sons, New York, 2004.

[12] B. Efron, T. Hastie, I. Johnstone, and R. Tibshirani, "Least angle regression," *The Annals of statistics*, vol. 32, no. 2, pp. 407–499, 2004.

[13] B. Sudret, "Global sensitivity analysis using polynomial chaos expansions," *Reliability Engineering & System Safety*, vol. 93, no. 7, pp. 964–979, 2008.

[14] T. Zhou, Z. Chen, W. D. Becker, S. L. Dvorak, and J. L. Prince, "Triangle impulse response (tir) calculation for lossy transmission line simulation," *IEEE Transactions on Advanced Packaging*, vol. 25, no. 2, pp. 311–319, May 2002.

[15] S. Marelli and B. Sudret, "UQLab: A framework for uncertainty quantification in matlab," in *Vulnerability Risk Analysis and Management, Proc. 2nd Int. Conf. on, Liverpool*, 2014, pp. 2554–2563.

[16] M. D. McKay, R. J. Beckman, and W. J. Conover, "A comparison of three methods for selecting values of input variables in the analysis of output from a computer code," *Technometrics*, vol. 42, no. 1, pp. 55–61, 2000.

Mourad Larbi received the M.S. degree in applied statistics from the University of Nice Sophia-Antipolis, Nice, France, in 2011, and the Ph.D. degree in electronics and telecommunications from the Institute of Electronics and Telecommunications of Rennes (IETR), Rennes, France, in 2016.

He is currently a Post-Doctoral Researcher with the Electromagnetic Compatibility Group, Department of Electronics and Telecommunications, Politecnico di Torino, Turin, Italy. His current research interests concern the risk analysis of signal propagation on interconnects in high-dimensional uncertainty quantification problems.

Igor S. Stievano (M'98 - SM'08) received the MS degree in electronic engineering and the PhD degree in electronics and communication engineering from the Politecnico di Torino, Torino, Italy, in 1996 and in 2001, respectively. Currently he is an Associate Professor of Circuit Theory with the Department of Electronics and Telecommunications, Politecnico di Torino. He is the author or coauthor of more than 130 papers published in international journals and conference proceedings. His research interests are in the field of electromagnetic compatibility and signal integrity, where he works on the modeling and characterization of linear and nonlinear circuit elements. His recent activities include the behavioral modeling of digital ICs, transmission lines and PLC channels, the modeling and simulation of switching converters and the development of stochastic methods for the statistical simulation of circuits and systems with the inclusion of the effects of device or manufacturing uncertainties.

Flavio G. Canavero (F'07) received the Master degree in electronic engineering from Politecnico (Technical University) of Torino, Italy, and the PhD degree from the Georgia Institute of Technology, Atlanta, USA, in 1986. Currently he is a Professor of Circuit Theory with the Department of Electronics and Telecommunications, Politecnico di Torino, where he serves also as the Director of the Doctoral School. He is an IEEE Fellow. He has been the Editor-in-Chief of IEEE Transactions on Electromagnetic Compatibility, vice president (V.P.) for Communication Services of the EMC Society and Chair of URSI Commission E. He has been the Co-Chair, with Professor Clayton Paul, of the first edition of Global EMC University in 2007. He received several Industry and IEEE Awards, including the prestigious Richard R. Stoddard Award for Outstanding Performance and the Honored Member Award of EMC Society. His research interests include signal integrity and EMC design issues, interconnect modeling, black-box characterization of digital integrated circuits, EMI and statistics in EMC.

Philippe Besnier (M'04, SM'10) received the diplôme d'ingénieur degree from Ecole Universitaire d'Ingénieurs de Lille (EUDIL), Lille, France, in 1990 and the Ph. D. degree in electronics from the university of Lille in 1993.

Following a one year period at ONERA, Meudon as an assistant scientist in the EMC division, he was with the Laboratory of Radio-Propagation and Electronics, University of Lille, as a researcher at the Centre National de la Recherche Scientifique (CNRS) from 1994 to 1997. From 1997 to 2002, Philippe Besnier was the director of Centre d'Etudes et de Recherches en Protection Electromagnétique (CERPEM): a non-for-profit organization for research, expertise and training in EMC and related activities, based in Laval, France. He also co-founded TEKCEM in 1998, a small business company specialized in turn-key systems for EMC measurements. Back to CNRS in 2002, he has been since then with the Institute of Electronics and Telecommunications of Rennes. Philippe Besnier was appointed as CNRS senior researcher (directeur de recherche) in 2013 an was co-head of the "antennas and microwave devices" department of IETR in 2012-2016. He headed the WAVES (electromagnetic waves in complex media) team during the first semester of 2017. Since July 2017, he is now deputy director of IETR. His research activities are mainly dedicated to interference analysis on cable harnesses (including electromagnetic topology), reverberation chambers, near-field probing and recently to the analysis of uncertainty quantification in EMC modeling.